Ansarino and Zorriasatein *Journal of Theoretical and Applied Physics* 2012, **6**:18
http://www.jtaphys.com/content/6/1/18

Journal of Theoretical and Applied Physics
a SpringerOpen Journal

RESEARCH Open Access

Density functional investigation of structures and energetics of pure and Sn-doped small lithium clusters

Masoud Ansarino* and Shahab Zorriasatein

Abstract

Ground state geometry, energetics, and bonding of pure Li_n ($n = 2-9$) and impure Li_nSn ($n = 1-8$) small clusters are investigated using the density functional theory. Introducing a single Sn impurity significantly changes the geometry of the host clusters for $n > 5$. Although the Sn atom is not trapped inside the cluster, it has the greatest coordination number among other atoms in the cluster. The analyses showed that the nearest neighbor bond lengths in Sn are approximately 10% shorter than those in Li. The results elucidate that the binding energy per atom in impure clusters is greater than that in pure clusters. Finally, it is shown that for Li_8 and Li_4Sn clusters that each have with eight valence electrons, the greater gap in the highest occupied molecular orbital and the lowest unoccupied molecular orbital results in a more stable cluster.

Keywords: Cluster, *ab initio*, DFT, MD, Ground state
PACs: 61.46. + w, 31.15.Ew, 31.15.Qg, 36.40.Qv

Background

The physical and chemical properties of materials such as melting point, heat capacity, flexibility, thermal and electrical conductivity, and magnetic and optical properties are known to be different in the nano field and the bulk state, and a strong dependence between these properties and the cluster's size has been established. This issue motivates the study of variation in geometry and energy in addition to the effects of cluster impurity on these parameters. Past studies on binary clusters that are composed of two types of elements revealed a number of interesting aspects including trapping of an impurity, changes in the equilibrium geometry, electronic structure, energetic properties, as well as bonding characteristics and stability of the doped clusters compare to the pure host.

Pure lithium and its metallic impurities are used in a wide range of applications, including batteries and accumulators, manufacturing of conductors, optical glasses, increasing brilliance of pigments, photographic industry, and synthesis of pharmaceutical and organic industry, which motivates additional investigation to better understand behavior of lithium nanoclusters.

Experimental studies on lithium clusters using photo ionization [1], evaporation [2], and Raman spectroscopy [3] have reported stability alternation in Li_n depending on even or odd value for n, with even-sized clusters being more stable. Also, the Li_8 and Li_{20} clusters (with 8 and 20 valence electrons) are shown to be more stable than other clusters.

Several properties of Li_n clusters, such as ground state (GS) and excited state (ES) geometries, electronic structure, binding and dissociation energies, ionization potentials, highest occupied molecular orbital and the lowest unoccupied molecular orbital (HOMO-LUMO) gap, and thermodynamics for different values of n, have been studied in the past [4-12]. Theoretical studies of lithium clusters with impurities such as Sn, Al, B, Na, Be, Mg, H, K, F, Si, C, and O have also been performed in the literature [13-39]. Most of these studies consider the lithium cluster as the host and investigate the effect of impurities. The results from studying impurity of Be in Li_n host cluster [33,34], Li in the Na_n clusters [29,30,32],

* Correspondence: m_ansarino@azad.ac.ir
Department of Physics, Faculty of Science, Islamic Azad University-South Tehran Branch, Tehran, Iran

Al in Li_n [12,17], and B in Li_n [23-25] indicate that, in general, an impurity with a smaller ionic radius and larger electronegativity prefers to be trapped in the host cluster [14]. On the other hand, the results from studying impurities of Mg in the host cluster of Li_n [33,34], Na in Li_n [29,31,33], K in Li_n [31,32], H in Li_n [36], Li in Si_n [38], Li in Al_n [18,22], Li in B_n [26], Li in Be_n [13], and Sn in Li_n [14-16] suggest that when the impurity stays on the surface of the host cluster, there is no relation between the atomic radius and the electronegativity of the guest and host atoms. Using molecular dynamic (MD) simulations, Joshi and Kanhere [7] studied the geometry of GS and ES as well as the thermodynamics of the Li_7 and Li_6Sn clusters. They observed a charge transferring from Li to Sn because of the significant difference in their electronegativity. Joshi and Kanhere [14], and Lee et al. [15] used DFT to study several properties of Li_nSn(n=1-9) clusters including the geometry of GS and ES, energetics, HOMO-LUMO gap, and electronic structure. They concluded that, among the cited clusters, Li_4Sn is the most stable cluster, that the Sn atom in the Li_n cluster is not trapped, and that charge transfer from Li to Sn is significant. Lee et al. [16] used MD to study the geometry, energetics, and bonds of $Li_{10-n}Sn(n=0-10)$ clusters and observed that a slight increase in Sn can alter the geometry of Li-rich clusters significantly.

The objective of this article is twofold. First, the geometry of GS and ES of pure Li_n clusters in the range of n = 2 to 9 are obtained to study energetics, bonds, and shapes of these clusters. Second, by substituting one tin atom in these clusters, we follow the same procedure that is performed for $Li_nSn\,(n=1-8)$ clusters to examine the effect of impurity on geometry, energy, and bonds of pure clusters.

Results and discussion

Figures 1 and 2 show the GS, the first and one of the interesting ES geometries for $Li_n\,(n=3-9)$ and $Li_nSn\,(n=2-8)$ clusters, respectively. The bond length of Li_2 and are 2.71 A and 2.76 A , respectively. The GS geometry of Li_3, an isosceles triangle with sides of 2.78 Å and a base of 3.31 Å, have been reported in the works of Gardet et al. and Jones et al. [4,5]. The ES structure of this cluster, which has 0.18 eV energy greater than GS, is linear [14,15]. The lowest lying structure of Li_2Sn cluster is an isosceles triangle with the Sn on its vertex. The bond length of Sn with Li atoms is 2.72 Å, while the bond length between Li atoms is 3.38 Å. In addition, the first ES of this cluster is linear.

The GS of Li_4 cluster [4,5,8] has the shape of a planar rhombus with sides of 3.00 Å. Replacing the Li atom with a single Sn atom in this cluster changes the shape of Li_3Sn to a deformed rhombus, in which the bond length of Sn with two Li atoms is 2.60 Å, with the third one being 2.69 A. This is a planar cluster with the first ES shape of a regular tetrahedron with a binding energy greater than 0.07 eV. The second ES of this cluster has the shape of an asterisk with a binding energy that is 0.25 eV greater than the GS. In this cluster, we observed the GS of Joshi and Kanhere [14] as the first ES. After Li_4 and Li_3Sn, the clusters are three-dimensional. The GS of Li_5 [4,5,9] has the shape of a triangular bipyramid, and its ES is planar with $\Delta E = 0.17$eV [9]. The lowest lying structure of Li_4Sn is a slightly distorted triangular bipyramid. This GS geometry has been reported in the works of Joshi and Kanhere and Shetty et al. [14,15]. Its first ES is a rectangular pyramid with 0.08 eV greater than GS. The GS of Li_6 [4,5,8,9,11] is a rectangular bipyramid and includes two rhombi that are perpendicular to each other. The first ES of this cluster is a pentagonal pyramid, while the second ES is planar with $\Delta E = 0.42$eV [9,11].

The lowest lying structure of Li_5Sn, which is a rectangular bipyramid, and its first ES with a 0.02eV greater energy have been reported [15]. The second

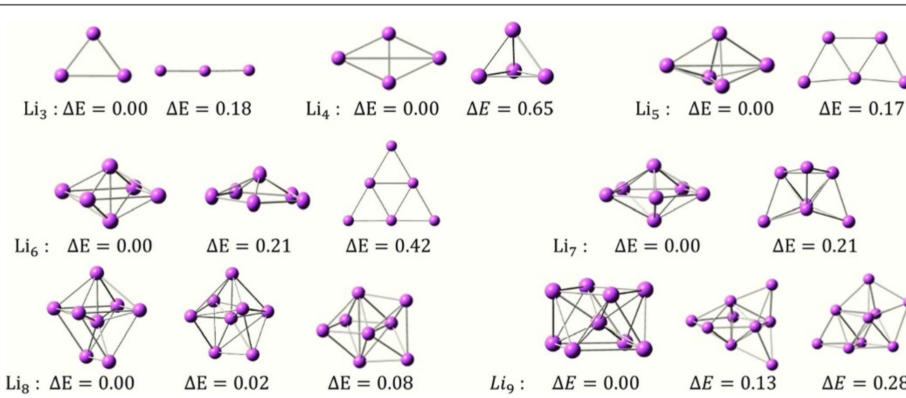

Figure 1 The ground state, first, and one of the interesting excited state geometries of Li_n(n=3–9) clusters. ΔE (in electron volt) is the difference in total energies.

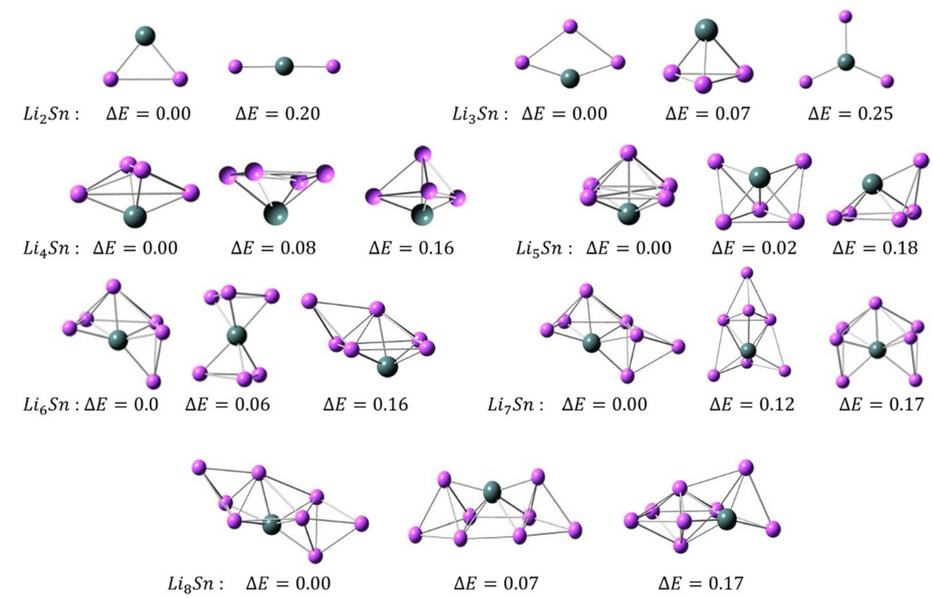

Figure 2 The ground state, first and one of the interesting excited-state geometries of $Li_nSn(n = 2–8)$ clusters. ΔE (in electron volt) is the difference in total energies.

ES with 0.18eV energy more than that in GS is a caped rectangular pyramid. Up to this stage, the geometry of either pure or impure clusters is almost similar, and the substitution of Sn atom has only slightly changed the shape of the host cluster. Hereafter, the existence of impure atom changes the geometry of the host cluster significantly. The GS of Li_7 cluster is a pentagonal bipyramid [4,5,7,9]. Its first ES with $\Delta E = 0.21$eV has been reported by Joshi and Kanhere [7]. The GS of Li_6Sn is a caped rectangular bipyramid and reported in the works of Joshi and Kanhere and Shetty et al. [7,14,15]. We observe that the first ES of this cluster with a 0.06eV greater energy has two tetrahedrons that connect through the vertex of Sn. Its tertiary ES with a binding energy of 0.16eV greater than the GS (the second ES is not shown in the figure) has been reported as the first ES [7]. The lowest lying geometry of Li_8 has the structure of Li_6 with two atoms added to the bottom. The same cluster with one trapped atom in it has been reported by Fournier et al. [6]. The Li_7Sn GS that has the same structure of Li_6Sn with one additional caped atom has not been reported so far. The Li_9 GS has the form of two rectangular pyramids that are connected through the vertex, creating a cage with an atom trapped in it [6]. The Li_8Sn GS has the same structure as Li_7Sn with another Li atom added to it. In fact, this cluster consists of two trigonal bipyramids that are connected through the vertex of Sn. The GS reported by Joshi and Kanhere [14] is one of the ES of this cluster. This ES has an additional 0.17-eV energy relative to its GS and the shape of a bi-caped pentagonal bipyramid.

It can be seen that Li_8 and Li_9 have trapped atoms. The comparison between Figures 1 and 2 shows that when the impurity of Sn is added to pure Li_n clusters, this impurity sets on the surface of the host cluster and changes its geometry. This change is especially significant for clusters with seven or more atoms.

The calculated coordination numbers (CN) for all atoms in impure Li_nSn clusters are shown in Table 1. To determine the CN, we assume the nearest neighbor distance of 3.3 Å. Up to Li_6Sn, the value of CN for the Sn atom is equal to the number of Li atoms in each cluster. For Li_7Sn and Li_8Sn, the Sn atom assume the maximum CN. The average value of bond length for the nearest

Table 1 Coordination numbers for the atoms in the GS geometries of $Li_nSn(n = 1–8)$

	Coordination numbers					
Cluster size	**1**	**2**	**3**	**4**	**5**	**6**
Li_1Sn	1 + Sn	0	0	0	0	0
Li_2Sn	2	Sn	0	0	0	0
Li_3Sn	0	2	1 + Sn	0	0	0
Li_4Sn	0	0	2	2 + Sn	0	0
Li_5Sn	0	4	0	0	1 + Sn	0
Li_6Sn	0	0	6	0	0	Sn
Li_7Sn	0	0	3	3	1	Sn
Li_8Sn	0	0	2	4	2	Sn

neighbors of Sn atom is approximately 10% less than that of Li atoms.

To analyze the stability of Li_n and Li_nSn clusters, the binding energy per atom (Eb), dissociation energy ($\Delta_1 E$), and second-order difference energy ($\Delta_2 E$) are calculated from the following equations:

$$E_b[Li_nSn] = \frac{nE[Li] + E[Sn] - E[Li_nSn]}{n+1} \quad (1)$$

$$\Delta_1 E[Li_nSn] = E[Li_{n-1}Sn] + E[Li] - E[Li_nSn] \quad (2)$$

$$\Delta_2 E[Li_nSn] = E[Li_{n+1}Sn] + E[Li_{n-1}Sn] - 2E[Li_nSn], \quad (3)$$

where $E[Li_n]$ is the total energy of the Li_n cluster. For pure clusters, Sn must be removed from all the terms. These energies for both pure and impure clusters have been reported in Tables 2 and 3. Figure 3 presents E_b for the GS of Li_n and Li_nSn as a function of the cluster size. The E_b increases by increasing the size of clusters. The E_b for impure clusters starts from 0.99eV and increases to 1.694 eV for Li_4Sn and, after a slight reduction, fluctuates in the range of 1.668 to 1.619eV.

It can be seen that the E_b for impure clusters is greater than that for pure clusters. The maximum difference between the E_b for pure and impure clusters is 0.69 eV, which is associated with the transition from Li_5 to Li_4Sn.

The energy differences $\Delta_1 E$ and $\Delta_2 E$ are sensitive indicators of relative stability. Figures 4 and 5 show $\Delta_1 E$ and $\Delta_2 E$ for pure and Sn-doped lithium clusters. As expected, with increasing cluster sizes, $\Delta_1 E$ and $\Delta_2 E$ show an odd-even behavior depending on the valance electrons. All clusters with even (odd) valence electron numbers have positive (negative) $\Delta_2 E$ values. Therefore, clusters with even valence electron numbers are more stable. The maximum value of $\Delta_2 E$ belongs to Li_8 for pure clusters and to Li_4Sn for impure clusters.

Another important indicator of cluster stability is the gap between HOMO-LUMO; with a larger HOMO-LUMO gap indicating higher stability. Figure 6 shows the HOMO-LUMO gap for pure and impure clusters of lithium. It can be verified that the even-odd fluctuation is dominant and that the HOMO-LUMO gap is greater for the clusters that do not have even valence electron numbers with unpaired electron. The pure and impure clusters Li_8 and Li_4Sn have the greatest HOMO-LUMO gap.

A comparison of Figures 4, 5, and 6 shows that Li_8, among the pure clusters; Li_4Sn, among the pure clusters; and Li_4Sn, among the impure clusters, are the most stable clusters. The relative stability of Li_8 and Li_4Sn clusters (both with eight valence electrons) is compatible with predictions from the shell model of clusters.

Table 2 Binding energy per atom (E_b), dissociation energy ($\Delta_1 E$), second-order difference energy ($\Delta_2 E$), and HOMO-LUMO gap of Li_n clusters

Li_n	E_b(eV/atom)	$\Delta_1 E$(eV)	$\Delta_2 E$(eV)	HOMO-LUMO gap(eV)
Li_2	0.729	0.726	0.718	-
Li_3	0.737	0.753	−0.865	0.249
Li_4	0.957	1.617	0.423	0.820
Li_5	1.004	1.194	−0.598	0.119
Li_6	1.136	1.792	0.183	0.648
Li_7	1.203	1.608	−0.513	0.545
Li_8	1.318	2.121	1.366	1.301
Li_9	1.255	0.755	-	0.077

Table 3 Binding energy per atom (E_b), dissociation energy ($\Delta_1 E$), second-order difference energy ($\Delta_2 E$), and HOMO-LUMO gap of Li_nSn clusters

Li_nSn	E_b(eV/atom)	$\Delta_1 E$(eV)	$\Delta_2 E$(eV)	HOMO-LUMO gap(eV)
Li_1Sn	0.987	0.978	0.635	-
Li_2Sn	1.332	2.017	−0.055	0.137
Li_3Sn	1.517	2.072	−0.330	0.759
Li_4Sn	1.694	2.402	0.879	1.058
Li_5Sn	1.666	1.523	−0.158	0.575
Li_6Sn	1.668	1.681	0.405	0.720
Li_7Sn	1.619	1.276	−0.462	0.310
Li_8Sn	1.632	1.738	-	1.001

Conclusions

The *ab initio* density functional method was applied to investigate systematic evolutionary trends in ground and

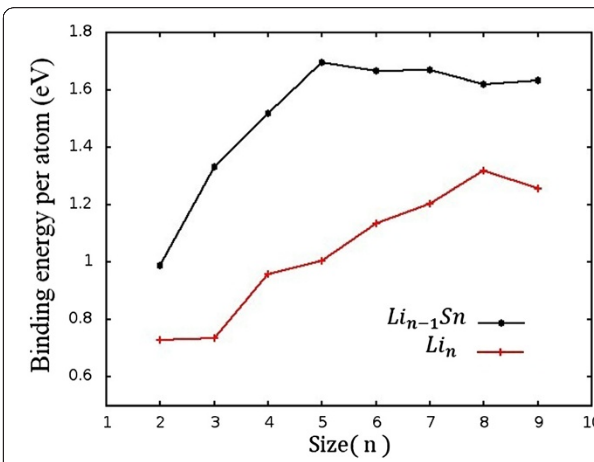

Figure 3 The binding energy per atom for Li_n and Li_n-1Sn(n=2-9) clusters.

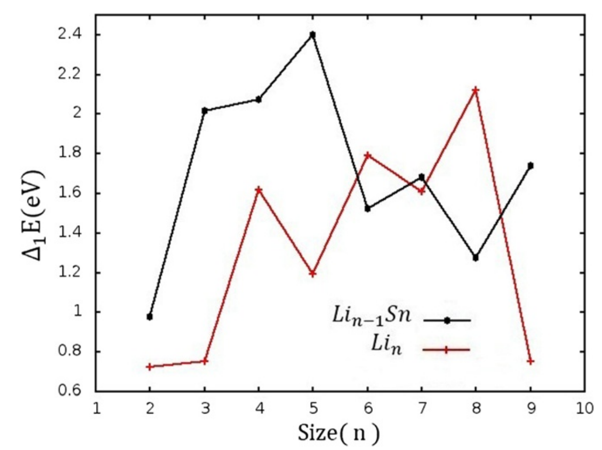

Figure 4 The dissociation energy for Li_n and $Li_{n-1}Sn$(n=2-9) clusters.

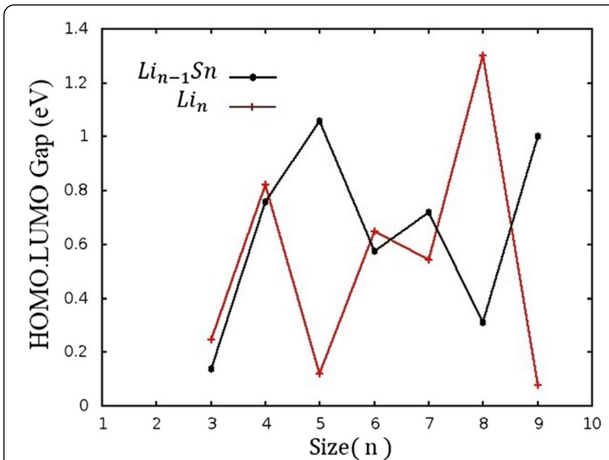

Figure 6 The HOMO-LUMO gap for Li_n and Li_n-1Sn(n=3-9) clusters.

excited state geometries and energies of Li_n $(n = 2-9)$ and Li_nSn $(n = 1-8)$ nanoclusters. The following conclusions are drawn from the results obtained:

1. The tetravalent Sn impurity changes the geometry of the host clusters. These changes become more significant after Li_5Sn. Since the Sn atom does not get trapped inside of the cluster, it was shown that the Sn atom prefers to go in a maximum coordination number. The average bond length for Sn-Li is 10% less than it is for Li-Li;
2. The introduction of Sn atom enhances the binding energy per atom as compared to the host clusters;
3. For pure and impure clusters, the odd-even behavior governs, Δ_1E, Δ_2E and HOMO-LUMO gap. The Li_8 and Li_4Sn clusters are most stable as they assume the highest HOMO-LUMO gaps and Δ_2E values.

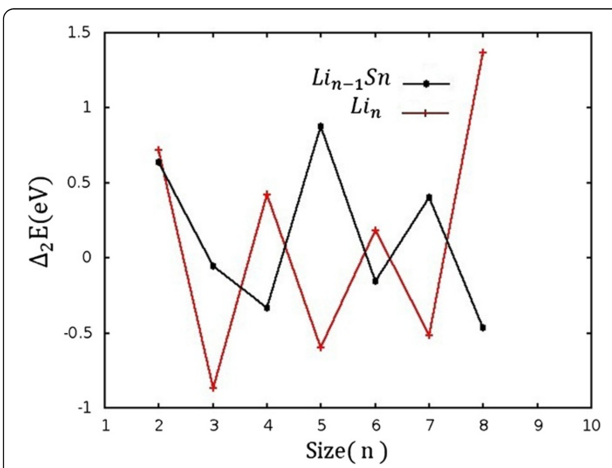

Figure 5 The second-order difference of energy for Li_n and Li_n-1Sn(n=2-8) clusters.

Methods

We have carried out *ab initio* density functional simulations using *V*anderbilt's ultrasoft pseudo potentials within the generalized gradient approximation (GGA) approach, as implemented in the *VA*SP package. We have optimized approximately 150 geometries for each of Li_n $(n = 2-9)$ clusters, 200 geometries for $n < 6$, and 400 for n>=6 for each impure Li_nSn(n=1-8) clusters. To obtain different initial configurations, we have carried out the following procedure. Constant temperature *ab initio* MD runs were carried out at five different temperatures, 300, 450, 600, 750, and 900 K. For pure clusters, each run simulated 45 ps that was completed in 15,000 MD steps of 3 fs. For impure clusters, 60 and 120 ps simulations were performed in 20,000 and 40000 MD steps of 3 fs for $n < 6$ and $n \geq 6$, respectively. These structures were then optimized using *ab initio* density functional method. For convergence in total energy, force, and cubic super cell length, we used 0.0001eV, 0.005 eV/Å, and 20 Å, respectively.

Competing interests

The author did not provide this information.

Acknowledgments

The support of this work, 'Effects of impurity on the Lithium cluster', is provided by the Islamic Azad University-South Tehran Branch.

Received: 10 May 2012 Accepted: 1 July 2012
Published: 30 August 2012

References

1. Dugourd, P, Rayane, D, Labastie, P, Vezin, B, Chevaleyer, J, Broyer, M: Chem Phys **197**, 433 (1992)
2. Brechignac, C, Bush, H, Cahuzac, P, Leygnier, J: J Chem Phys **101**, 6992 (1994)
3. Kornathand, A, Kaufmann, A: J Chem Phys **118**, 6957 (2003)
4. Gardet, G, Rogemond, F, Chermette, H: J Chem Phys **105**, 9933 (1996)
5. Jones, RO, Lichtenstein, AI, Hutter, J: J Chem Phys **106**, 4566 (1997)
6. Fournier, R, Cheng, JBY, Wong, A: J Chem Phys **119**, 9444 (2003)
7. Joshi, K, Kanhere, D.G: J Chem Phys **119**, 12301 (2003)

8. Grassi, A, Lombardo, GM, Angilella, GGN, March, NH, Pucci, R: J Chem Phys **120**, 11615 (2004)
9. Alexandrova, AN, Boldyrev, AI: J Chem Theory Comput **1**, 566 (2005)
10. Wheeler, SE, Schaefer, HF: J Chem Phys **122**, 204328 (2005)
11. Temelso, B, Sherrill, CD: J Chem Phys **122**, 064315 (2005)
12. Lee, MS, Gowtham, S, He, H, Lau, KC, Pan, L, Kanhere, DG: Phys Rev B **74**, 245412 (2006)
13. Lei, XL, Zhao, WJ, Ge, GX, Yang, Z, Yan, YL, Luo, YH: Physica B **403**, 653 (2008)
14. Joshi, K, Kanhere, DG: Phys Rev A **65**, 043203 (2002).
15. Shetty, S, Pal, S, Kanhere, DG: J Chem Phys **118**, 7288 (2003)
16. Lee, MS, Kanhere, DG, Joshi, K: Phys Rev A **72**, 015201 (2005)
17. Cheng, HP, Barnett, RN, Landman, U: Phys Rev B. **48**, 1820 (1993)
18. Majumder, C, Das, GP, Kulshrestha, SK, Shah, V, Kanhere, DG: Chem Phys Letter **261**, 515 (1996)
19. Chacko, S, Deshpande, M, Kanhere, DG: Phys Rev B **64**, 155409 (2001)
20. Akola, J, Manninen, M: Phys Rev B **65**, 245424 (2002)
21. Chacko, S, Kanhere, DG, Paranjape, VV: Phys Rev A **70**, 023204 (2004)
22. Tai, T.B., Nhat, P.V., Nguyen, M.T.: Phys Chem Chem Phys **12**, 11477 (2010)
23. Li, Y, Wu, D, Sun, CC: J Comput Chem **28**, 1677 (2007)
24. Li, Y, Liu, YJ, Wu, D, Li, ZR: Phys Chem Chem Phys **11**, 5703 (2009)
25. Tai, TB, Nguyen, MT: Chem Phys Letter **489**, 75 (2010)
26. Tai, TB, Nguyen, MT: Chem Phys **375**, 35 (2010)
27. Dahlseid, TA, Kappes, M, Pople, JA, Ratner, MA: J Chem Phys **96**, 4924 (1992)
28. Koutecky, VB, Gaus, J, Guest, MF, Koutecky, J: J Chem Phys **96**, 4934 (1992)
29. Deshpande, MD, Kanhere, DG, Panat, PV, Vasiliev, I, Martin, RM: Phys Rev A **65**, 053204 (2002)
30. Deshpande, MD, Kanhere, DG, Vasiliev, I, Martin, RM: Phys Rev A **65**, 033202 (2002)
31. Jiang, ZY, Lee, KH, Li, ST, Chu, SY: Int J Mass Spec **253**, 104 (2006)
32. Fournier, R: J Comput MethodSc Eng **8**, 331 (2008)
33. Deshpande, M, Dhavale, A, Zope, RR, Chacko, S, Kanhere, DG: Phys Rev A **62**, 063202 (2000)
34. Baruah, T., Kanhere, D.G., Zope, R.R.: Phys Rev A **63**, 063202 (2001)
35. Fuentealba, P, Savin, A: J Phys Chem A **105**, 11531 (2001)
36. Wheeler, SE, Sattelmeyer, KW, Schleyer, PVR, Schaefer, HF: J Chem Phys **120**, 4683 (2004)
37. Hakete, N, Yokoyama, K, Tanaka, H, Kudo, H: J Molec Struc (Theochem) **577**, 55 (2002)
38. Wang, H, Lu, WC, Li, ZS, Sun, CC: J Molec Struc (Theochem) **730**, 263 (2005)
39. Li, G, Li, X, Wang, C, Ma, G: J Molec Struc (Theochem) **910**, 50 (2009)

doi:10.1186/2251-7235-6-18
Cite this article as: Ansarino and Zorriasatein: **Density functional investigation of structures and energetics of pure and Sn-doped small lithium clusters.** *Journal of Theoretical and Applied Physics* 2012 **6**:18.